PAPER

Seebeck effect studies in the charge density wave state of organic conductor α-(BEDT–TTF)$_2$KHg(SCN)$_4$

To cite this article: D Krstovska *et al* 2021 *Phys. Scr.* **96** 125734

Physica Scripta

PAPER

Seebeck effect studies in the charge density wave state of organic conductor α-(BEDT–TTF)$_2$KHg(SCN)$_4$

RECEIVED
18 October 2021

REVISED
12 December 2021

ACCEPTED FOR PUBLICATION
22 December 2021

PUBLISHED
31 December 2021

D Krstovska[1], E S Choi[2] and E Steven[2,3]

[1] Ss. Cyril and Methodius University, Faculty of Natural Sciences and Mathematics, Arhimedova 3, 1000 Skopje, Macedonia
[2] National High Magnetic Field Laboratory, Florida State University, Tallahassee, FL 32310, United States of America
[3] Emmerich Research Center, Jakarta Utara, DKI Jakarta 14450, Indonesia

E-mail: danica@pmf.ukim.mk **and** krstovska@magnet.fsu.edu

Keywords: interlayer Seebeck effect, quasi-two dimensional organic conductor, charge density wave, magnetic quantum oscillations

Abstract

Angular, magnetic field and temperature dependence of the interlayer Seebeck effect of the multiband organic conductor $\alpha - (BEDT - TTF)_2KHg(SCN)_4$ is experimentally studied at temperatures down to 0.55 K and fields up to 31 T in a wide range of angles. The background magnetic field and angular component of the Seebeck effect as well as the magnetic quantum oscillations that originate from the closed Fermi surface orbits are analyzed. The background interlayer Seebeck effect components show that above certain tilt angle of the magnetic field and above the kink field there is another CDW state in $\alpha - (BEDT - TTF)_2KHg(SCN)_4$, between previously known CDW_0 and CDW_x states, in agreement with magnetoresistance and magnetization studies in this material. Our observations show that this state possesses some of the properties of the CDW_0 state. The Fermi surface in the third CDW state is still reconstructed but less imperfectly nested as expected as this state develops above the kink field. The temperature dependence of the interlayer Seebeck effect reveals that this state is developed at temperatures below 3 K and at field orientations around the second AMRO maximum. In addition, for the first time, a detailed $T - \theta$ phase diagram of $\alpha - (BEDT - TTF)_2KHg(SCN)_4$ based purely on Seebeck effect measurements is presented. We find that other states and transitions, beside the CDW states, also exist in a given temperature and angular range that have not been previously reported. These observations change the whole picture about the transport processes in the organic conductor $\alpha - (BEDT - TTF)_2KHg(SCN)_4$ and allow to better understand the complex nature of the CDW order in this and similar compounds.

1. Introduction

The investigation of electron transport phenomena in multilayered organic structures is especially significant because of their great importance for applied sciences. Conducting organic molecular crystals based on the BEDT-TTF and TMTSF molecules are novel low-dimensional electronic systems [1]. The family $\alpha - (BEDT - TTF)_2MHg(SCN)_4$ [M = K, Rb, Tl] are of particular interest because they have a rich phase diagram and coexisting quasi-one dimensional and quasi-two dimensional Fermi surface (FS) [2, 3]. Metallic, superconducting, and density wave phases are possible, depending on temperature, pressure, magnetic field, and anion type [4]. At ambient pressure, the family with M = K, Rb, Tl undergo a transition from a metal to a charge density wave (CDW) phase at a temperature $T_{CDW} = 8$, 10, and 12 K, respectively caused by the Peierls-type nesting instability of the open Fermi sheets [5, 6]. On passing through the so-called 'kink-field' transition at $B \sim 23$ T (for M = K), the CDW is removed and is replaced by a metallic phase with a FS consisting of a quasi-two dimensional (q2D) hole cylinder, known as the α pocket, and a pair of quasi-one dimensional (qlD) electronic sheets [7]. The low-dimensional character of the organic conductors leads to important consequences in their response to a magnetic field. In fact, qualitatively new effects, in particular related to the field orientation, have been found in these materials [1, 8].

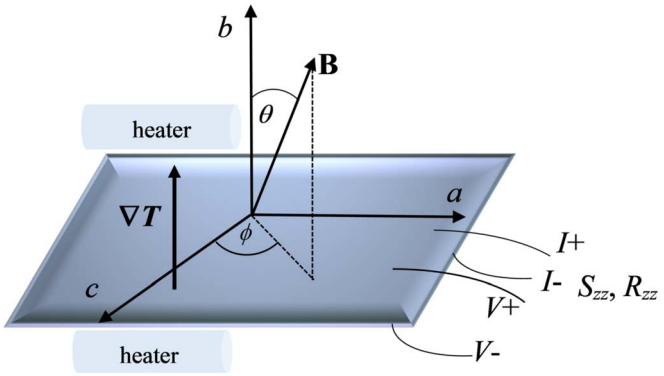

Figure 1. The experimental setup for the interlayer magnetoresistance and Seebeck effect measurements in the organic conductor $\alpha - (BEDT - TTF)_2KHg(SCN)_4$ as a function of the magnetic field and its orientation. The temperature gradient ∇T is along the less conducting axis, b − axis of the conductor, perpendicular to the Q2D conducting ac plane. The magnetic field **B** is rotated for angle θ from the b-axis to the ac-plane at a fixed azimuthal angle of $\phi = 37^\circ$ from the c-axis.

The organic compound central to this investigation is still arousing considerable interest due to existence of multiple field-induced CDW phases [9]. The already existing studies on properties of $\alpha - (BEDT - TTF)_2KHg(SCN)_4$ show that for a field perpendicular to the most conducting plane, its electronic structure can be separated into three regimes; the normal metallic state, CDW_0 and CDW_x [10, 11]. Each electronic regime of $\alpha - (BEDT - TTF)_2KHg(SCN)_4$ is characterized with a specific dependence of the magnetoresistance with respect to field orientation. At temperatures below the transition temperature $T_p = 8$ K and kink field $B_K \sim 23$ T, angular dependent magnetoresistance oscillations with sharp dips similar to those in some quasi-one dimensional organic conductors [12, 13] are observed. On contrary, at temperatures above T_p and fields above B_K the angular magnetoresistance oscillations are rather quasi-two dimensional with peaks periodic in $\tan\theta$ [14, 15].

The magnetoresistance and magnetization of the Q2D organic conductor $\alpha - (BEDT - TTF)_2KHg(SCN)_4$ in the CDW state were studied by many authors (see [5, 8] and references therein). Apart from that, the Seebeck and Nernst effect in this material have been studied both theoretically and experimentally only in a number of works [16–18]. However, such studies are of great importance since thermomagnetic phenomena are significantly more sensitive to the electron energy spectrum of the degenerate conductors than the galvanomagnetic effects. Therefore, they might give more information about the charge carriers involved in the transport processes as well as the values of the parameters that shape the FS.

In this paper, we study the low temperature angular and magnetic field dependence of the interlayer Seebeck effect (or interlayer magnetothermopower) in the ground state of the organic conductor $\alpha - (BEDT - TTF)_2KHg(SCN)_4$. In addition, we examine the temperature dependence of the Seebeck effect as a function of magnetic field and its orientation. The most significant results of the present investigation include: confirmation of previous reports that in $\alpha - (BEDT - TTF)_2KHg(SCN)_4$ there is another low temperature CDW state at angles above $\theta = 40^\circ$ and fields above the kink field; first determination of the $T - \theta$ phase diagram of $\alpha - (BEDT - TTF)_2KHg(SCN)_4$ based purely on interlayer Seebeck effect measurements; the study of the onset of magnetic breakdown effects via the Seebeck effect, and the measurement of quantum oscillations in the Seebeck effect.

2. Experiment

The single-crystal sample in this study was grown using conventional electrochemical crystallization techniques, and was mounted on a rotating platform with a precision better than a degree. Two pairs of Au wires were attached to the sample along the b- axis on the opposite sides of the ac-planes of the sample by carbon paste for both the resistance and Seebeck effect measurements. The resistance was measured by a conventional 4-probe low frequency lock-in technique. The sample was positioned between two quartz blocks (figure 1), which were heated by sinusoidal heating currents with an oscillation frequency f_0 and phase difference $\pi/2$ to establish a small temperature gradient along the b-axis. The corresponding temperature gradient (∇T) and the thermal emf with $2f_0$ oscillation frequency were measured for the magnetothermopower signal. The method for Seebeck effect measurements used in this work is detailed elsewhere [19]. The direction of the magnetic field $\mathbf{B} = (B\sin\theta\cos\phi,\ B\sin\theta\sin\phi,\ B\cos\theta)$ is measured with respect to polar θ (b-axis to ac-plane) and fixed azimuthal angle $\phi = 37^\circ$ (with respect to c-axis in the ac-plane) as shown in figure 1.

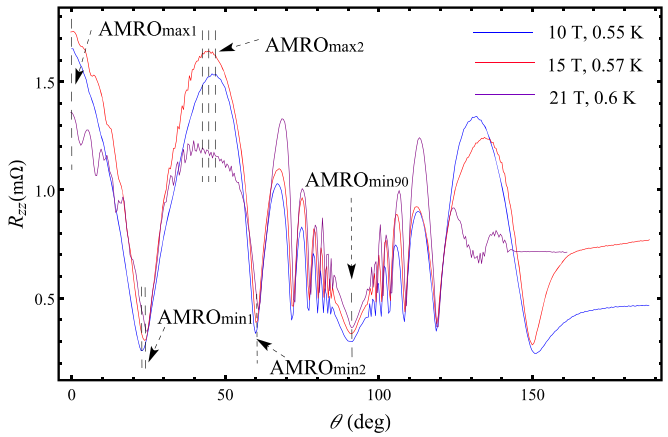

Figure 2. Angular magnetoresistance oscillations in $\alpha - (BEDT - TTF)_2KHg(SCN)_4$ for several fields: $B = 10$ T, 15 T, 21 T and temperatures: $T = 0.55$ K, 0.57 K, 0.6 K, respectively. The Shubnikov-de Haas quantum oscillations are visible at high fields above $B = 10$ T and angles below 60°. The positions of some of the AMRO maxima and minima are indicated by dashed lines.

3. Results and Discussion

Although the organic conductor under consideration is characterized by a complex ground state which is field and temperature dependent, many aspects of a standard, semi-classical Boltzmann treatment provide a good explanation of the data without taking into account the unconventional transport mechanisms.

Below a detailed description of the evolution of the Seebeck effect with the magnetic field strength, its orientation and the temperature in the two-band organic conductor $\alpha - (BEDT - TTF)_2KHg(SCN)_4$ is presented with emphasis on its behaviour in the charge density wave state. Along the $z-$ axis the FS is slightly corrugated as a result of the finite dispersion between the layers perpendicular to the $xy-$ plane. In the $xy-$ plane the FS consists of open sheets and closed cylindrical parts, from which q1D and q2D behavior of the electronic system evolves, respectively.

3.1. Angular-dependent oscillations of the magnetoresistance and Seebeck effect

The angular oscillations are characteristic of the kinetic and thermoelectric coefficients of layered organic conductors and are absent in isotropic metals. They are associated with the charge carriers motion on the cylindrical closed pockets and quasi-planar sheets of the FS in a tilted magnetic field. As charge carriers move across the FS under the influence of the magnetic field their component of velocity in a given direction varies as they drift along the various FS parts so that the total velocity remains perpendicular to the FS at all times. The periodic oscillations of the transport coefficients emerge when a constant magnetic field is turned from the direction normal to conducting layers toward the plane of the layers.

In a two-band organic conductor an external magnetic field affects differently the motion of charge carriers whose states belong to the weakly corrugated cylinder and corrugated plane sheets of the FS. Thus, the presence of open planar sheets of the FS is most easily revealed in a conductor placed in a magnetic field. Consequently, the contributions from different conducting channels can be detected and separated more accurately by studying the magnetothermoelectric effects in such conductors.

3.1.1. Angular magnetoresistance oscillations

Figure 2 shows the angular magnetoresistance oscillations (AMROs) in $\alpha - (BEDT - TTF)_2KHg(SCN)_4$ for several fields: 10 T, 15 T, 21 T and temperatures: 0.55 K, 0.57 K, 0.6 K in the CDW_0 state. The Shubnikov-de Haas (SdH) quantum oscillations, associated with Landau quantization of the closed orbit FS are observed superimposed on the AMROs for higher fields above $B = 10$ T and at angles below $\theta = 60°$. The SdH oscillations are mainly due to the closed α orbit of frequency $F_\alpha = 673$ T, which in $\alpha - (BEDT - TTF)_2KHg(SCN)_4$ emerges above $B = 8$ T, and are most prominent at high fields above 20 T and angles below 60° as evident in purple curve in figure 2. The angular constrain for the SdH oscillations is due to the the elongation of the elliptic α orbit with increasing angle. A series of dips are observed at the so-called Lebed magic angles $\theta = \theta_n$ [1] given by $\tan(\theta_n)\cos(\phi - \phi_0) = \tan(\theta_0) + n\Delta_0$ where $\tan(\theta_n) = 0.5$, $\Delta_0 = 1.25$, $\phi_0 = 27°$ and $n = 0, \pm 1, \pm 2, \ldots$ in agreement with earlier experiments.

The appearance of the sharp dips in the AMROs is a confirmation that at low temperatures and below the kink field the main contribution to the observed angular dependence comes from the electrons belonging on the open orbits on the Fermi surface. The obvious observation from figure 2 is that the AMRO maxima and minima

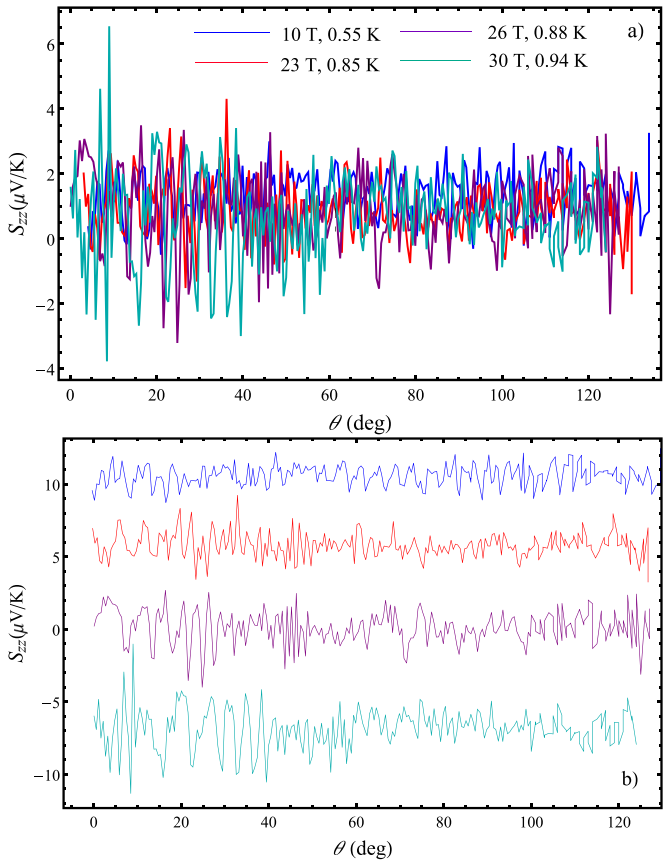

Figure 3. (a) Angular dependence of the total interlayer Seebeck effect, $S_{zz}(\theta)$, in $\alpha - (BEDT - TTF)_2KHg(SCN)_4$ for several fields: $B = 10$ T, 23 T, 26 T, 30 T and temperatures: $T = 0.54$ K, 0.85 K, 0.88 K, 0.94 K, respectively. There is a decrease in the amplitude of the Seebeck effect quantum oscillations for angles above 60° but the oscillations are present in the whole range of angles. (b) The same curves are presented shifted from each other for more clarity of the evolution of angular quantum oscillations.

slightly shift their angular position towards higher angles with increasing both the magnetic field strength and temperature.

According to the semiclassical Boltzmann transport theory a similarity between the magnetoresistance and Seebeck effect should be expected as the interlayer Seebeck effect S_{zz} is a product of the interlayer resistivity ρ_{zz} and the corresponding thermoelectric coefficient α_{zz}, $S_{zz} = \rho_{zz}\alpha_{zz}$, with the interlayer thermoelectric coefficient obtained by the Mott formula $\alpha_{zz} = \frac{\pi^2 k_B T}{3e} \frac{d\sigma_{zz}(\varepsilon)}{d\varepsilon}|_{\varepsilon=\mu}$, where μ is the chemical potential of the electron system and $\sigma_{zz}(\varepsilon)$ is the energy-dependent interlayer electrical conductivity. This allows to further analyze the angular behavior of the Seebeck effect on the base of the semiclassical description of the transport.

3.1.2. Angular oscillations of the interlayer Seebeck effect

Figure 3 shows the angular dependence of the total interlayer Seebeck effect in $\alpha - (BEDT - TTF)_2KHg(SCN)_4$ for several fields: $B = 10$ T, 23 T, 26 T, 30 T and temperatures: $T = 0.54$ K, 0.85 K, 0.88 K, 0.94 K, respectively.

The interlayer Seebeck effect shows rather complex angular behavior at low temperatures in the CDW state compared to that at higher temperatures, for example at 4 K, previously studied in [18]. In comparison, there are pronounced angular quantum oscillations at low temperature that are not seen at higher temperature due to the thermal smearing of the FS with increasing temperature. In addition, at low temperatures, the angular quantum oscillations of the interlayer Seebeck effect are present in the whole angular range and fields $B \geqslant 10$ T compared to those of the interlayer magnetoresistance (figure 2) which are observed up to a certain angle of approximately 60° and only at high fields. The amplitude of the Seebeck effect quantum oscillations decreases above 60° and fields above the kink field B_K but are still present. The observed suppression of the quantum oscillations is associated not only with the elongation of the closed α orbits with increasing angle but also with the existence of different field-induced phases in $\alpha - (BEDT - TTF)_2KHg(SCN)_4$ depending on the field strength and tilt angle. In regards to that, in order to analyze the angular behavior of the interlayer Seebeck effect in $\alpha - (BEDT - TTF)_2KHg(SCN)_4$ properly we relate it with the corresponding CDW state and in correlation with the interlayer magnetoresistance behaviour. Additionally, we are also studying the behavior of the

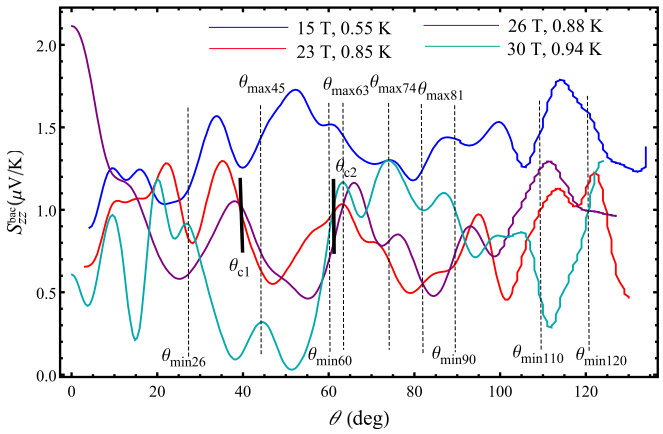

Figure 4. Angular dependence of the background interlayer Seebeck effect, $S_{zz}^{bac}(\theta)$, in $\alpha - (BEDT - TTF)_2KHg(SCN)_4$ obtained after filtering out the quantum oscillations component at the same fields and temperatures as in figure 3. The expected general trend is decreasing of the Seebeck effect with increasing angle but at low temperatures the Seebeck effect exhibits a rather complex behaviour very different than that observed at high temperatures. The mid-angle positions of the resonant-like features in the angular Seebeck effect coinciding with the locations of the AMRO maxima and minima are indicated by dashed lines.

interlayer Seebeck effect with magnetic field and temperature to reveal the boundaries of existence of each of the different CDW states in this organic conductor for more accurate presentation and analysis of the experimental results as well as for determination of the phase diagram. In reference to that, we present in figure 4 the angular dependence of the background interlayer Seebeck effect which is more sensitive to the Fermi surface topology than the quantum oscillation component and hence determines the main angular behavior of the Seebeck effect.

The background Seebeck effect in $\alpha - (BEDT - TTF)_2KHg(SCN)_4$ is an oscillating function of the angle and should decrease with increasing angle due to the decrease of the induced longitudinal voltage with the rotation of the field away from the $b -$ axis. However, exceptions are seen in the high field Seebeck effect (above the kink field) which is increasing with rotation of the field above certain angle ($\theta_{c1} \sim 40^\circ$ for $B = 26$ T and $\theta_{c2} \sim 60^\circ$ for $B = 30$ T). The Seebeck effect is the largest at $\theta = 0^\circ$ as expected as this is the direction along the temperature gradient. Indeed, for $\theta = 0^\circ$, $\mathbf{B} \| \nabla T$, and the generated longitudinal voltage that determines the Seebeck effect is the largest. With rotation of the magnetic field away from the $b -$ axis the longitudinal voltage, and consequently the Seebeck effect, decreases. Thus, the expected general trend in the angular dependence is that the Seebeck effect decreases with increasing angle towards $\theta = 90^\circ$ (for fields in the conducting plane) and than continues to increase again with further increasing angle. Exactly this kind of behaviour was previously observed at higher temperature ($T = 4$ K) in the CDW_0, CDW_x and metallic state [18]. Also at $T = 4$ K, the interlayer Seebeck effect is the largest in the CDW_0 while decreases with the transition of the system into the CDW_x and metallic state. However, this is not a case at low temperatures, especially in the CDW state. At low temperatures $S_{zz}^{bac}(\theta)$ displays a rather complex oscillatory behaviour than the simple decreasing with the angle. On the other hand, we find that a common feature of the Seebeck effect for both low and high temperature is its resonant-like behaviour (two close to each other extremes in the angular dependence), which is more prominent at low temperatures. At high temperatures not only that the resonant-like features are less pronounced but are present up to a certain angle $\theta \sim 50^\circ$ and only in the CDW_0 state, i.e., below the kink field B_K [18]. Our results show that at low temperatures the resonant-like features exist in the whole angular range as well as in the CDW_x state, i.e., above the kink field B_K. Similar as in the case of $T = 4$ K we find that the mid-angle between the two extremes coincides with the locations of the AMRO maxima or minima. Most importantly, at low temperatures below 1 K and below the kink field, in the CDW_0 state (blue curve), all of the mid-angle positions coincide with the AMRO maxima or minima whereas for fields above the kink field this pattern is seen only at certain angles larger than the critical angle θ_c (as seen in the purple and cyan curve in figure 4). In the CDW_x state (represented by the red curve and the purple and green curves below θ_{c1} and θ_{c2}, respectively) the positions of the mid-angle between the extremes and the AMROs positions do not coincide implying that the wavevector Q of this CDW state is not affected by the magnetic field rotation but is only dependent on the magnetic field magnitude.

The changes in the Seebeck effect around the critical angle θ_c might be correlated with existence of another CDW state, between already existing CDW_0 and CDW_x states, whose wavevector Q is angle-dependent. Support to this claim is also the fact that our results reveal a larger interlayer Seebeck effect at high fields above the critical angle θ_c (opposite from the expected decrease of the interlayer Seebeck effect with increasing angle) that is field and temperature dependent. The third CDW state was previously found to exist by the magnetoresistance and magnetization measurements at low temperatures in [20]. To the best of our knowledge, [20] is the only evidence

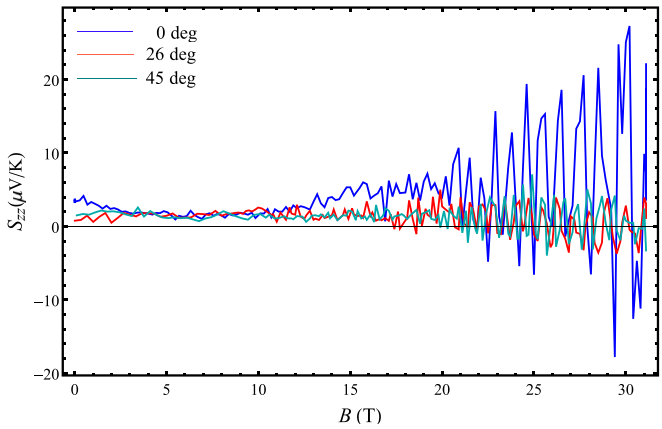

Figure 5. Magnetic field dependence of the total interlayer Seebeck effect in $\alpha - (BEDT - TTF)_2KHg(SCN)_4$ obtained at $T = 0.6$ K and different angles: $\theta = 0°, 26°, 45°$ that correspond to the first maximum, first minimum and second maximum in AMROs, respectively.

for existence of a third CDW state in this organic conductor. It was found that the material exhibits at least three low-temperature electronic subphases with the third one, the CDW_y state, appearing for angles $\theta \geqslant \theta_c \simeq 45°$ of the magnetic field with respect to the $b-$ axis as a result of the interplay between Pauli and orbital effects. Our results on the interlayer Seebeck effect indicate that indeed there are changes in the electronic structure of the conductor that occur above $\theta \sim 40°$. Also, we can see from figure 4 that at angles above θ_c, where the third CDW state is expected, the mid-angle positions again coincide with some of the AMRO maxima or minima which is not a case for the CDW_x (red curve). This indicates that the third CDW state is more similar in its properties to the ground CDW_0 state. This is further confirmed with the magnetic field and temperature dependence of the interlayer Seebeck effect discussed below. For what concerns the angular Seebeck effect represented by the red curve in figure 4 we see that the mid-angle positions do not coincide with AMROs locations for smaller angles but they do coincide for higher angles $\theta > 70°$. The reason is that this angular dependence is obtained for measurements of the Seebeck effect around the kink field for the given temperature ($T = 0.85$ K) and hence most probably both CDW_x and CDW_y state affect the observed behaviour; the CDW_x below $\theta \sim 70°$ and the CDW_y above this angle up to $\theta_{\min} = 90°$.

3.2. Magnetic field dependence of the interlayer Seebeck effect

Figure 5 shows the magnetic field dependence of the total interlayer Seebeck effect in $\alpha - (BEDT - TTF)_2 KHg(SCN)_4$ obtained at $T = 0.6$ K and for three different angles: $\theta = 0°, 26°, 45°$. These angles are intentionally chosen for obtaining the magnetic field dependence as they correspond to the orientation of the magnetic field along the first maximum, first minimum and second maximum in the AMROs (figure 2), respectively. This allows to reveal the corresponding behaviour of the Seebeck effect with the magnetic field for different orientations as well as to determine the angular dependence of the kink field B_K at low temperatures.

The magnetic quantum oscillations of the Seebeck effect are clearly visible above $B = 8$ T with a highest amplitude for a magnetic field orientation along the least conducting direction in $\alpha - (BEDT - TTF)_2 KHg(SCN)_4$, $b-$ axis (figure 6). When the field is rotated away from this direction their amplitude is significantly reduced especially above the kink field. Although the second harmonic of α frequency in $\alpha - (BEDT - TTF)_2KHg(SCN)_4$ appears below 2 K the observed magnetic quantum oscillations of the Seebeck effect are mainly due to the electrons on the closed α orbit. In fact, the 2αfrequency is present in the Fast Fourier Transform (FFT) spectrum for the given tilt angles, shown in figure 7, but with significantly lower amplitude than that of the α frequency, especially it is much lower for field rotation away from the direction of the temperature gradient. Therefore, in general, the 2αfrequency does not modulate the quantum oscillations with the exception of the high fields above $B = 27$ T where the splitting of the quantum oscillations occurs and the waveform is obtained as a combination of both α and 2αfrequency.

The FFT spectrum of the magnetic quantum oscillations obtained in a field range $B = 12 - 30$ T reveals that the α frequency is dominant in the oscillations and it shifts towards higher values as the magnetic field is rotated in the ba plane. The corresponding fundamental frequency for the given field direction from the $b-$ axis is $F_{\alpha 1} = 673$ T for $\theta = 0°$, $F_{\alpha 2} = 845$ T for $\theta = 26°$ and $F_{\alpha 3} = 1135$ T for $\theta = 45°$. The frequency of α orbit should follow the $1/\cos\theta$ scaling indicating a cylindrical Fermi surface. However, we obtain slightly higher values for the α frequency than those expected from the $1/\cos\theta$ dependence. Usually this can result from the misalignment of the angle during the measurements. However, in our case the AMRO data (figure 2) show that

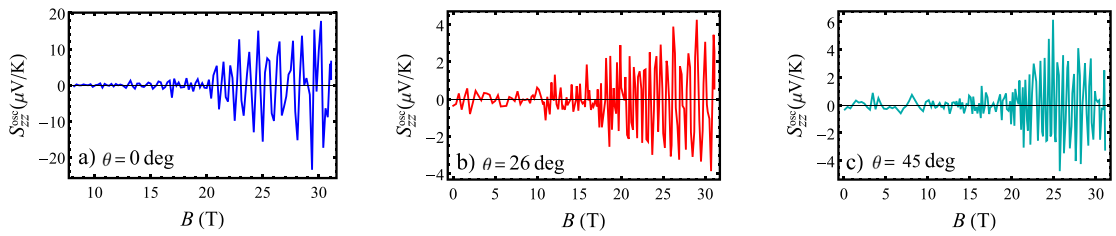

Figure 6. Magnetic quantum oscillations of the interlayer Seebeck effect in $\alpha - (BEDT - TTF)_2KHg(SCN)_4$, $S_{zz}^{osc}(B)$, obtained for $T = 0.6$ K and the same angles as in figure 5. The oscillations are seen above $B = 10$ T and are most prominent for the magnetic field parallel to the least conducting axis, $b -$ axis.

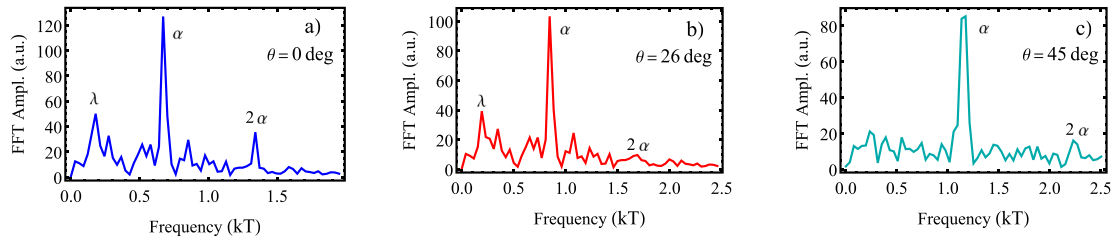

Figure 7. FFT spectrum of the magnetic quantum oscillations of the interlayer Seebeck effect obtained in a field range $B = 12 - 30$ T and for the same angles as in figure 5: (a) $\theta = 0°$, (b) $\theta = 26°$ and (c) $\theta = 45°$.

the positions of the angular magnetoresistance dips are at the Lebed magic angles which indicates a correct angle. This is further supported by the fact that $F_\alpha = 673$ T at 0° is close to previously reported value for this organic conductor. Furthermore, the values obtained for the magnetic breakdown filed B_{MB} are close to each other for the given field orientations. Experimentally, there is always a possibility of random diffusion of heat along the sample due to even a small misalignment between the heat current and the crystal axes, which can be a source of a transverse voltage leading to an increased thermal diffusion of the carriers in the sample. Thus, for the magnetothermoelectric measurements the in-plane components could be significant and their mixing can in general affect the overall behaviour of the interlayer Seebeck signal. In regards to that, we find that the angular dependence of the α orbit frequency for our results fits well with $a + b/\cos\theta$ dependence (a and b are constants) where the first term would account for the carriers' thermal diffusion. This is plotted in figure 8.

The suppression of the magnetic quantum oscillations of the interlayer Seebeck effect at higher angles is associated with the decrease of the amplitude of the fundamental α orbit with tilting the magnetic field away from the $b -$ axis. The α-oscillations are result of the magnetic breakdown (MB) effect. Using the kink field values for the $CDW_0 \rightarrow CDW_x$ phase transition at each angle one can calculate the energy gap between the open and closed orbits of the Fermi surface, $\Delta \sim \pi\mu_B B_K$, which allows to estimate the corresponding MB field, $B_{MB} \sim \Delta^2 m_c/\hbar e\varepsilon_F$ at each field orientation. Here, $\varepsilon_F = 35$ meV is the Fermi energy, $m_c = 1.5me$ is the effective cyclotron mass and e is the elementary charge. This allows to study the onset of the MB effects with the angle via the quantum oscillations of the Seebeck effect. Thus, for kink filed of $B_K = 22, 24, 25$ T at tilt angles of the magnetic field $\theta = 0°, 26°, 45°$ (as obtained from the field dependence of the background Seebeck effect in figure 8 below) the following values for the energy gap are obtained $\Delta = 4, 4.36, 4.54$ meV, respectively. The obtained values for Δ yield MB field of $B_{MB} = 5.95, 7.1, 7.7$ T, respectively. It is obvious that the energy gap of the $CDW_0 \rightarrow CDW_x$ phase transition becomes larger as the field is rotated away from the least conducting direction in $\alpha - (BEDT - TTF)_2KHg(SCN)_4$ making it more difficult for the electrons to traverse it. Consequently, the formation of the MB α orbits and the magnetic quantum oscillations associated with these orbit shift towards higher fields with tilting the field from the normal to the layers.

In addition to α and 2αfrequency, the FFT spectrum reveals existence of λ frequency at low fields associated with formation of small closed pockets on the FS after reconstruction due to quantum interference effect. This frequency was previously reported in the low temperature quantum oscillations of the magnetoresistance and magnetization [21] as well as in the interlayer Seebeck effect for magnetic field along the direction of the temperature gradient [22]. We find from our angular measurements of the Seebeck effect quantum oscillations that the λ frequency is present not only for $\theta = 0°$ with $F_\lambda \sim 180$ T (Figure 7(a)), in agreement with previous reports, but it is also still visible for tilt angles close to the temperature gradient direction, $F_\lambda \sim 192$ T for $\theta = 26°$ (Figure 7(b)) whereas it is absent for higher angles above $\theta = 40°$ (figure 7(c)). This indicates that the slow

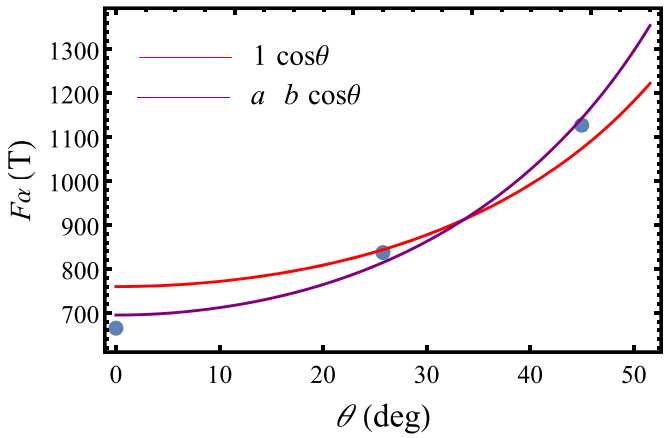

Figure 8. Angular dependence of the fundamental α frequency obtained from the interlayer Seebeck effect measurements. The red curve is for the $1/\cos\theta$ and the purple curve is obtained by fitting with the $a + b/\cos\theta$ dependence. A reasonable fit of the α frequency values is obtained with the $a + b/\cos\theta$ dependence most probably due to thermal diffusion of the charge carriers.

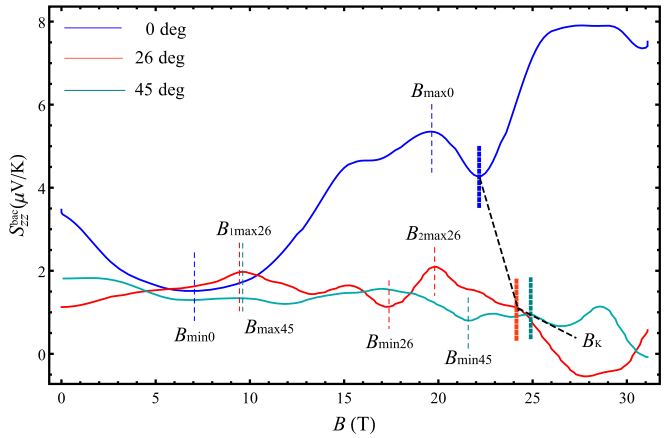

Figure 9. Magnetic field dependence of the background Seebeck effect in $\alpha - (BEDT - TTF)_2KHg(SCN)_4$, $S_{zz}^{bac}(B)$, obtained at the same angles as in figure 5 after filtering out the quantum oscillation component. The minimum and maximum features that appear in the field dependence at different field orientations as well as the kink field B_K that defines the high-field regime where the zero-field state CDW_0 is transformed into the CDW_x are indicated. The dashed black line shows the shift of the kink field towards higher values with increasing tilt angle.

oscillations are present in the Seebeck effect waveform for rotations of the field away from the temperature direction. Moreover, since the slow oscillations originate form the small closed pockets formed on the Fermi surface after the reconstruction, in the CDW_0 state, our results show that these small pockets are present in the reconstructed FS only up to a certain tilt angle of the magnetic field, above which there are only open FS orbits, in agreement with the vanishing λ frequency with rotation of the field close to the Q2D planes. As the λ frequency is absent for angles above $\theta = 40^\circ$ (figure 7(c)) it follows that in the third CDW state the number of small closed orbits is significantly lower indicating that in this state the FS is still reconstructed (although this state occurs above the kink field where the original unreconstructed FS is expected) but less imperfectly nested than that in the CDW_0 state. Thus, the observations revealed from the magnetic quantum oscillations of the interlayer Seebeck effect give more detailed insights into the parameters that shape the Fermi surface of $\alpha - (BEDT - TTF)_2KHg(SCN)_4$ below and above the kink field. Hence, our results will provide obtaining more accurate representation of the FS shape in different CDW states in $\alpha - (BEDT - TTF)_2KHg(SCN)_4$.

In figure 9 we present the magnetic field dependence of the background Seebeck effect in $\alpha - (BEDT - TTF)_2KHg(SCN)_4$ obtained at the same angles as in figure 5 after filtering out the quantum oscillations component from the total interlayer Seebeck effect. The main behaviour of the total Seebeck effect is determined by the magnetic field dependence of its background component as expected as this component of the Seebeck effect is very sensitive to the change of the Fermi surface topology. The changes in the background interlayer Seebeck effect are correlated to the change of the electronic structure, associated with the electron-hole asymmetry at the transition.

Our study reveals features in the background Seebeck effect, in particular maxima and minima which appear at a certain field with tilting the magnetic field at the position of the AMRO maxima or minima that are not clearly visible in the total Seebeck effect. Furthermore, the kink field B_K displays a nontrivial angular dependence with tilting the field from the $b-$ axis. In the CDW_0 state, below B_K, the Seebeck effect is predominantly positive with a prominent change in the behavior with increasing field and angle. For a magnetic field along the direction of the temperature gradient ($b-$ axis), figure 9 reveals a development of a pronounced feature in a form of an upturn around 20 T preceded by a broad dip at $B_S = B_{\min 0} \sim 7$ T (blue curve). Interestingly, the appearance of a specific feature in a form of a dip followed by an upturn in the Seebeck effect of $\alpha - (BEDT - TTF)_2KHg(SCN)_4$ is a behavior previously observed in the Seebeck coefficient of the orthorhombic high-Tc cuprate YBCO [23]. Most strikingly, there is another dip in the Seebeck effect at high field around $B_K \sim 22$ T followed by another upturn. We see that at low temperature there appear successive upturns at a certain field that produce dips near the magnetic breakdown field $B_{MB} \sim 6$ T and again around the kink field $B_K \sim 22$ T for $\theta = 0°$. The changes in the Seebeck effect are usually attributed to the change of the electronic band structure of the material, associated with the change in the electron-hole asymmetry due to a transition of the system into another ordered state. Therefore, the observed features in the Seebeck effect are indicative of a prominent change in the electronic configuration, i.e., signify a presence of a pronounced FS reconstruction at low temperatures. Moreover, the observed features in the Seebeck effect are confirmation for establishing a certain type of CDW order in $\alpha - (BEDT - TTF)_2KHg(SCN)_4$ similarly as detected in YBCO [23]. Actually, it is well know that a CDW order indeed develops in this organic conductor at low temperatures below 8 K but the significance of our results is that they allow to distinguish between different types of a CDW order by following the Seebeck effect behaviour in a magnetic field. We associate the first dip with the appearance of the CDW_0 state with a zero-field wavevector. As the onset magnetic field B_S for this state is slightly above the magnetic breakdown field $B_{MB} \sim 6$ T it is evident that the CDW_0 state indeed emerges due to FS reconstruction as a result of the magnetic breakdown effect in agreement with previous findings [5, 21]. In regards to that, the positive (negative) Seebeck effect signifies presence of a hole (electron) pocket caused by the FS reconstruction related to CDW modulations. The other dip around the kink field $B_K \sim 22$ T leads to appearance of another upturn around $B = 25$ T followed by a saturation of the Seebeck effect at high field that is not seen in the low field state. The behavior of the Seebeck effect above B_K is rather different than that below B_K. The second dip is more narrow followed by a sudden increase in the Seebeck effect right above B_K with almost no change in the magnitude at fields above $B = 26$ T. This implies that another CDW state is realized with a field independent Seebeck effect. This is the high field state of $\alpha - (BEDT - TTF)_2KHg(SCN)_4$, CDW_x, with a field dependent wavevector. The field independent Seebeck effect in the high field state of $\alpha - (BEDT - TTF)_2KHg(SCN)_4$ was also observed at $T = 4$ K [17].

We find that with rotation of the magnetic field away from the $b-$ axis the Seebeck effect is significantly reduced in magnitude and the features are much less pronounced than those when the field is along the $b-$ axis. This is, however, expected as when the field is rotated away from the direction of the temperature gradient the Seebeck effect decreases as a result of a much smaller longitudinal voltage. Moreover, the dips in the Seebeck effect at low field is much less prominent for both AMRO minimum $\theta = 26°$ (red curve) and AMRO maximum $\theta = 45°$ (cyan curve) direction of the magnetic field but the upturn is present around $B_{1\,\max 26} \sim 9.5$ T and $B_{\max 45} \sim 10$ T, respectively. Above $B_{1\,\max 26}$ there are other smaller upturns preceded by dips in $S_{zz}^{bac}(B)$ for $\theta = 26°$ while it decreases above $B \sim 20$ T. For AMRO minimum position the interlayer Seebeck effect changes sign from positive to negative at $B \sim 26$ T above which is field independent. Since this behaviour is similar to the one in case of $\theta = 0°$ it indicates that the CDW_x state is again realized above $B_K \sim 24$ T for a magnetic field orientation at AMRO minimum but this one is characterized with an electron-like transport unlike the CDW_x state for $\theta = 0°$ where holes are dominant charge carriers. This indicates that the FS is still imperfectly nested with the rotation of the field at the direction of the AMRO minimum with a difference that the small closed orbits in the CDW_x state for this direction are electron-like. For $\theta = 45°$, the interlayer Seebeck effect is the smallest in magnitude with further decrease for fields above 17 T up to the kink field indicating that the CDW_0 state is weakened. The more interesting part is the interlayer Seebeck effect behaviour above the kink field $B_K \sim 25$ T. Indeed, it does not resemble neither of the previous two cases but rather continues to display behaviour in a form of a small dip followed by a small upturn at high field. This is an indicator that for angles above $\theta = 40°$ another CDW state emerges with different order than the previous two CDW states. This is in agreement with above revealed from the angular dependence of the interlayer Seebeck effect as well as with magnetoresistance and magnetization studies in this material [20]. Moreover, the observed behaviour in a form of a dip followed by an upturn in the interlayer Seebeck effect in the third CDW state indicates that some properties of this state are similar to those of the CDW_0 state (since these features are most prominent in the CDW_0 state). This further indicates that in the third CDW state the FS would still be imperfectly nested (i.e., still reconstructed) but to a lesser extent than in the CDW_0 state since the features observed in the magnetic field

dependence of the interlayer Seebeck effect are reduced in magnitude above the kink field with the rotation of the field.

3.3. Temperature dependence of the interlayer Seebeck effect

We have also performed Seebeck effect measurements with the temperature in order to further confirm the development of the new state in $\alpha - (BEDT - TTF)_2KHg(SCN)_4$ as well as to establish the exact temperature interval in which each of the CDW states exists for a given magnetic field strength and orientation.

Usually, the Seebeck and Nernst effect are a complex mixture of phenomena which can be difficult to interpret, unless specific aspects of the system under consideration change drastically. In the frame of the semiclassical Boltzmann transport theory, a similarity between the magnetic field, angular and temperature dependence of the Seebeck effect and magnetoresistance should be expected. Therefore, it is instructive to discuss our experimental results in the context of previous findings on temperature dependence of the magnetoresistance [24]. It was shown that below 15 K, the temperature dependence of the magnetoresistance is metallic for magnetic field orientation corresponding to an AMRO minimum and nonmetallic at all other field orientations which is a behaviour common to any system with either quasi-one or quasi-two dimensional AMROs. This behavior has been explained in terms of the semiclassical Boltzmann theory taking into account the contributions from both quasi-one dimensional planar Fermi sheets and quasi-two dimensional cylinder without the use of a non-Fermi liquid description. It is found that in the CDW_0 state, when the field direction corresponds to an AMRO minimum, the sample resistance is metallic. Deviations from this orientation results in nonmetallic behavior in the temperature dependence which is more pronounced as the field orientation approaches AMRO maxima. The observed different behaviour of magnetoresistance is associated with change of effective dimensionality with field orientation. Most interestingly, in the CDW_x state, there is a reentrant metallic behavior of the magnetoresistance below 3 K for positions corresponding to AMRO maxima.

In connection to our results, we find that the Seebeck effect exhibits more complex behaviour than that of magnetoresistance [25]. The evolution of different phases in a restricted temperature interval is evident form figure 10, moreover, the temperature dependence confirms the existence of the new CDW phase, CDW_y phase, and the coexistence of the CDW and metallic state at both AMRO maxima and AMRO minima orientations of the magnetic field. Figure 10 shows the evolution of the total interlayer Seebeck effect in $\alpha - (BEDT - TTF)_2KHg(SCN)_4$ with the temperature, $S_{zz}(T)$, for different tilt angles and magnetic field strengths. Our results reveal substantial differences in the $T-$ dependent profiles of the Seebeck effect depending on whether the magnetic field is oriented along AMRO maximum or AMRO minimum.

For a moderate magnetic field of 15 T applied parallel to the temperature gradient ($\theta = 0^\circ$) there exist only two different states, CDW_0 and normal state, over a restricted temperature interval (figure 10(a)). Indeed, below 8.5 K a CDW_0 state is developed with a $S_{zz}(T) = A + B/T + C/T^2$ dependence, where A, B and C are constants. Above 8.5 K there is a normal state with $S_{zz}(T) = D + ET$ dependence, where D and E are constants. Here the first constant term is regarded as the contribution of electronic interaction and the second term is carriers' diffusion component. Obviously, the case for $\theta = 0^\circ$ is distinct than the other field orientations as it is characterized with two strictly separated states, CDW_0 and metallic state, with a smooth crossover from metallic to CDW_0 at a transition temperature $T = 8.5$ K (figure 10(a)). The reason for that might be that the FS is completely reconstructed with the transition into the CDW_0 state when a temperature of 8.5 K is reached. The Seebeck effect is positive at temperatures up to 11 K (it reaches zero at 11 K which corresponds to perfect FS nesting) although decreasing with increasing temperature. This indicates that the imperfect FS nesting begins below 11 K and is completed at 8.5 K at which the system smoothly transitions into the CDW_0 state.

For a magnetic field of 20 T oriented along the first AMRO minimum ($\theta = 26^\circ$) the temperature dependence of the Seebeck effect displays a more complex behaviour (figure 10(b)). Interestingly, in this case, the CDW_0 state emerges below 5 K with a $S_{zz}(T) = F + G/T + H/T^2$ dependence, where F, G and H are constants, while in the interval 5 K-8.5 K $S_{zz}(T) = I/T^2$ (I is a constant) which is a behaviour describing the phase transition from metallic to the low temperature CDW_0 state. Above 8.5 K there exists a mixed state with a $S_{zz}(T) \sim J + KT + L/T^2$ dependence (J, K and L are constants). It is evident that when the magnetic field is oriented at the first AMRO minimum location the whole picture changes significantly since with rotation of the magnetic field the FS topology changes as seen from change in the evolution of states with the temperature (figure 10(b)). In this case what is suppose to be a normal metallic state above 8.5 K is now a mixed state which is a combination of a metallic behaviour and another one revealed within the emphasized phase transition occurring below 8.5 K down to 5 K. The Seebeck effect is zero for 8.5 K, it is negative above and positive below this temperature. Here the imperfect FS nesting occurs at 8.5 K while the FS reconstruction is completed at around 5 K. This is an indication that the obtained $1/T^2$ behaviour for the Seebeck effect is due to the nesting features in the electron energy spectrum. Once the FS reconstruction is completed, below 5 K, the same CDW_0 state is realized as the one obtained for $\theta = 0^\circ$ in figure 10(a). The observed temperature dependence of Seebeck

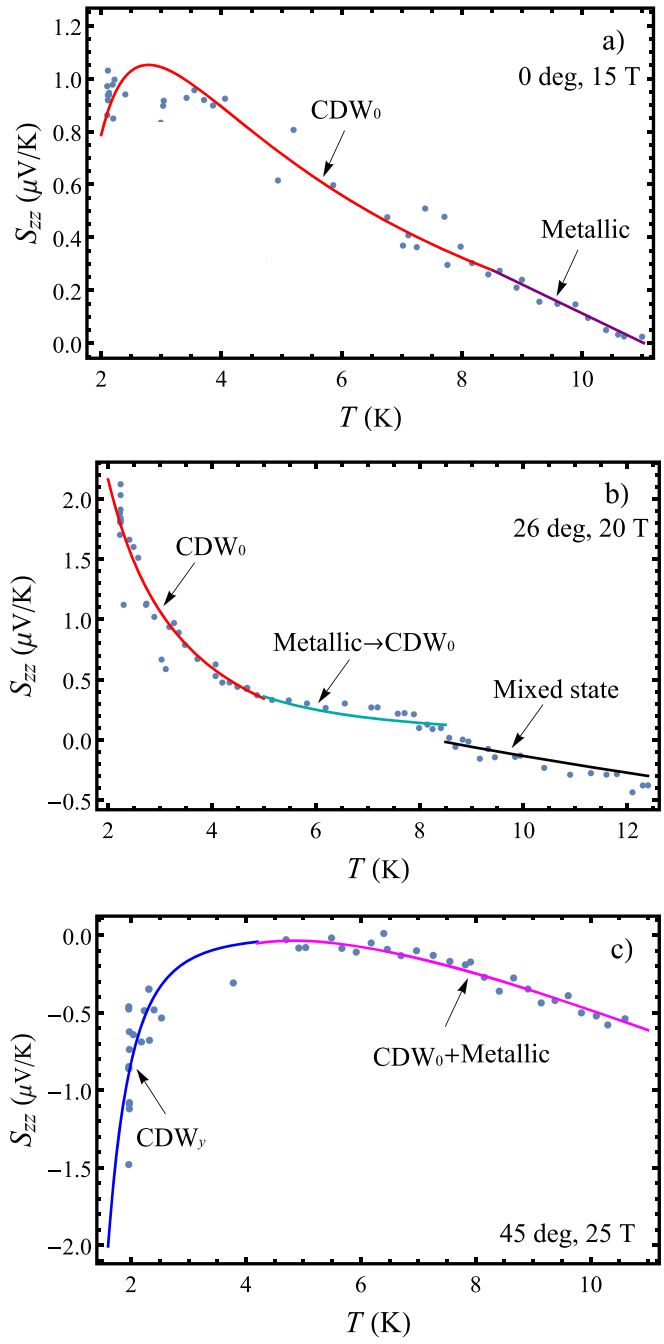

Figure 10. Temperature dependence of the interlayer Seebeck effect, $S_{zz}(T)$, in $\alpha - (BEDT - TTF)_2KHg(SCN)_4$ obtained for different magnetic field strengths and orientations: a) $\theta = 0°$, $B = 15$ T; b) $\theta = 26°$, $B = 20$ T and c) $\theta = 45°$, $B = 25$ T. The prominent change in the T dependence of the Seebeck effect is evident with increasing tilt angle and magnetic field strength.

effect shows that the influence of FS nesting (the $1/T^2$ term in $S_{zz}(T)$) is also reflected in the CDW_0 state at low temperatures while thermal activation over a band gap gives a $1/T$ dependence. The latter is associated with the phonon drag effect due to the electron-phonon coupling. This indicates that beside the FS nesting, electron-phonon coupling also has its own contribution in the formation of the CDW_0 state in $\alpha - (BEDT - TTF)_2KHg(SCN)_4$.

At a high magnetic field of 25 T oriented along the AMRO maximum ($\theta = 45°$) (figure 10(c)) the sample Seebeck effect is proportional to a M/T^4 (M is a constant) dependence below 4 K. Above 4 K a new state which is a combination of normal metallic state and CDW_0 state with a $S_{zz}(T) = N + OT + P/T + R/T^2$ dependence (N, O, P, R are constants) is realized. The newly observed behaviour of the Seebeck effect ($\sim 1/T^4$) below 4 K, although this temperature dependence is more reliable below 3 K, describes the third CDW state occurring just below $\theta = 45°$ and on the edge of the kink field transition $B_K = 25$ T. Interestingly, with the rotation of the magnetic field above $\theta \sim 40°$ the CDW_0 state still survives together with the metallic one even at temperatures

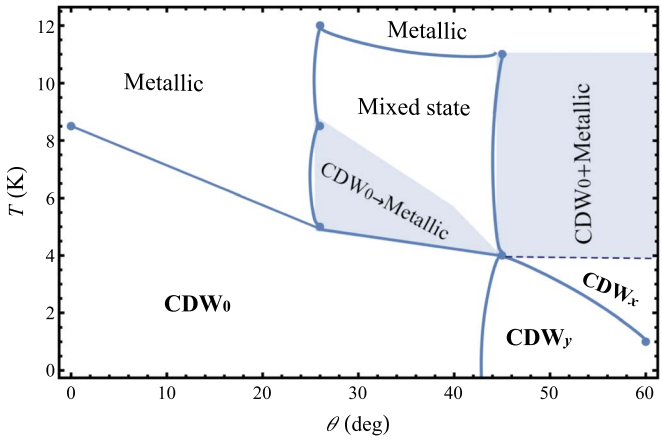

Figure 11. The tentative $T-\theta$ phase diagram of $\alpha-(BEDT-TTF)_2KHg(SCN)_4$. Solid lines are guides to the eyes. The three possible CDW regions and the metallic state are indicated in a given temperature and angular interval. The metallic $\rightarrow CDW_0$ transition which is most probably triggered when the magnetic field orientation is along the first AMRO minimum, the possible mixed state as well as the existence of a combination of CDW_0 and metallic state are presented. The temperature-angular interval for the CDW_x state is provisional as it has been established from the angular dependence of the Seebeck effect at low temperatures obtained in this work (figure 4) and the one in [18] for $T=4$ K (figure 3(a)).

above 8.5 K, where only the metallic state is expected. This indicates that the angular effects are indeed significant in the distribution of the CDW order in this organic conductor. Consequently, the rotation of the magnetic field causes the FS reconstruction (accompanied with appearance of small closed pockets on the sides of the FS as well as new open orbits) to happen at higher temperatures and hence the presence of the CDW_0 state is detected at temperatures slightly above the transition temperature.

We note that the temperature dependence of the magnetoresistance shows that it is metallic for magnetic field orientation corresponding to an AMRO minimum and nonmetallic at all other field orientations [24]. On contrary, the temperature dependence of the Seebeck effect shows that the nonmetallic behaviour is observed for both AMRO maximum and minimum (except for $\theta=0^\circ$) which is a rather expected behaviour as the AMRO maxima and minima coincide with the mid-angle positions in the Seebeck angular resonant-like features (figure 4).

The proposed $T-\theta$ phase diagram in figure 11 (which has not been given by far) shows the possible CDW regions in $\alpha-(BEDT-TTF)_2KHg(SCN)_4$. In addition, the phase diagram reveals presence of other states within a given temperature and angular range. The metallic $\rightarrow CDW_0$ transition most probably occurs for field orientations between the first AMRO minimum ($\theta=26^\circ$) and second AMRO maximum ($\theta=45^\circ$) within a certain temperature interval above which there is a mixed state for the same range of angles. With increasing angle the CDW_y state appears above $\theta\sim40^\circ$ and only at low temperatures below 4 K. On the other hand, with increasing temperature above 4 K this state is replaced by another one which demonstrates properties similar to both CDW_0 and metallic state.

4. Conclusions

Detailed studies of the interlayer Seebeck effect of organic conductor $\alpha-(BEDT-TTF)_2KHg(SCN)_4$ as a function of temperature, magnetic field strength, and field orientation are reported. Our observations reveal that the properties of this quasi-two dimensional organic conductor are far more complex than previously anticipated, especially in its response to a magnetic field orientation. We find that the formation of the CDW_0 state is mainly due to the FS reconstruction as a result of the magnetic breakdown effect since the onset magnetic field for this state is near the magnetic breakdown field. However, the electron-phonon coupling might be also an important mechanism in formation of the CDW_0 state in $\alpha-(BEDT-TTF)_2KHg(SCN)_4$ as evident from the temperature dependence of the interlayer Seebeck effect. Our studies confirm and advance previous findings on the existing of several different CDW states in the organic conductor $\alpha-(BEDT-TTF)_2KHg(SCN)_4$ and reveal that in this system the electronic structure is far more complex than previously anticipated. We find that a third CDW state develops at low temperatures below 3 K at angles above $\theta=40^\circ$ and fields above the kink field. At these angles and fields the high field CDW_x state with a field dependent wavevector is replaced by the CDW_y state with an angle dependent wavevector. In addition, we find that the third CDW state resembles some of the properties of the CDW_0 state but the FS is less imperfectly nested than in the CDW_0 state. The temperature

measurements reveal substantial differences in the $T-$ dependent profiles of the Seebeck effect depending on whether the magnetic field is oriented along AMRO maximum or AMRO minimum. This allows to specify the temperature interval of existence of each of the CDW states for a given magnetic field strength and orientation as well as to reveal the presence of other possible states and transitions in $\alpha-(\mathrm{BEDT}-\mathrm{TTF})_2\mathrm{KHg(SCN)_4}$ that have not been previously detected by magnetoresistance and/or magnetization measurements.

Acknowledgments

This work was performed at the National High Magnetic Field Laboratory, supported by NSF DMR-0654118, by the State of Florida, and by the DOE.

Data availability statement

All data that support the findings of this study are included within the article (and any supplementary files).

ORCID iDs

D Krstovska https://orcid.org/0000-0002-0546-2445

References

[1] Lebed A (ed) 2008 *The Physics of Organic Superconductors and Conductors* (Heidelberg: Springer)
[2] Mori H, Tanaka S, Oshima M, Saito G, Mori T, Maruyama Y and Inokuchi H 1990 Crystal and electronic structures of (BEDT-TTF)$_2$[MHg(SCN)$_4$] (M = K and NH$_4$) *Bull. Chem. Soc. Jpn.* **63** 2183–8
[3] Rousseau R, Doublet M-L, Canadell E, Shibaeva R P, Khasanov S S, Rozenberg L P, Kushch N D and Yagubskii E B 1996 Electronic structure of the α-(BEDT-TTF)$_2$MHg(XCN)$_4$ (M=Tl, K, NH$_4$; X = S, Se) and related phases. Synthesis and crystal structure of the new stable organic metal α-(BEDT-TTF)$_2$TlHg(Se$_{1-x}$S$_x$CN)$_4$ (x=0.125) *J. Phys. I France* **6** 1527
[4] Brooks J S 1993 Organic conductors and superconductors: New directions in the solid state *MRS Bull.* **18** 29
[5] Kartsovnik M V 2008 *Layered Organic Conductors in Strong Magnetic Fields in Physics of Organic Superconductors and Conductors* (Heidelberg: Springer) 185
[6] Foury-Leylekian P, Pouget J-P, Lee Y-J, Nieminen R M, Ordejón P and Canadell E 2010 Density-wave instability in $\alpha-(BEDT-TTF)_2KHg(SCN)_4$ studied by x-ray diffuse scattering and by first-principles calculations *Phys. Rev.* B **82** 134116
[7] Harrison N, Balicas L, Brooks J S and Tokumoto M 2000 Critical state in a low-dimensional metal induced by strong magnetic fields *Phys. Rev.* B **62** 14212
[8] Kartsovnik M V 2004 High magnetic fields: a tool for studying electronic properties of layered organic metals *Chem. Rev.* **104** 5737–45
[9] Andres D, Kartsovnik M V, Grigoriev P D, Biberacher W and Müller H 2003 Orbital quantization in the high-magnetic-field state of a charge-density-wave system *Phys. Rev.* B **68** 201101(R)
[10] Biškup N, Perenboom J A A J, Brooks J S and Qualls J S 1998 Argument for charge density wave sub-phases in the ground state of $\alpha-(BEDT-TTF)_2KHg(SCN)_4$ *Solid State Comm.* **107** 503–5
[11] Kartsovnik M V, Biberacher W, Steep E, Christ P, Andres K, Jansen A G M and Müller H 1997 High-field studies of the H-T phase diagram of $\alpha-(BEDT-TTF)_2KHg(SCN)_4$ *Synth. Metals* **86** 1933–4
[12] Osada T, Yagi R, Kawasumi A, Kagoshima S, Miura N, Oshima M and Saito G 1990 High-field magnetotransport and Fermi-surface topology in the novel quasi-two-dimensional organic conductor bis(ethylenedithiolo)tetrathiafulvalenium mercuric postassium thiocyanate, $(BEDT-TTF)_2KHg(SCN)_4$ *Phys. Rev.* B **41** 5428(R)
[13] Sasaki T and Toyota N 1995 Mysterious ground states in the organic conductor $\alpha-(BEDT-TTF)_2KHg(SCN)_4$: Mixed SDW and CDW? *Synth. Metals* **70** 849–52
[14] House A A, Blundell S J, Honold M M, Singleton J, Perenboom J A A J, Hayes W, Kurmoo M and Day P 1996 Phase boundary in the dimensionality of angle-dependent magnetoresistance oscillations in the charge-transfer salt $\alpha-(\mathrm{BEDT}-\mathrm{TTF})_2\mathrm{KHg(SCN)_4}$ *J. Phys. Condens. Matter* **8** 8829
[15] Ishiguro T, Yamaji J and Saito G 1998 *Organic Superconductors* (Berlin, Heildeberg, New York: Springer)
[16] Choi E S, Brooks J S and Qualls J S 2002 Magnetothermopower study of the quasi-two-dimensional organic conductor $\alpha-(BEDT-TTF)_2KHg(SCN)_4$ *Phys. Rev.* B **65** 205119
[17] Krstovska D, Steven E, Choi E S and Brooks J S 2011 Angular dependent magnetothermopower of $\alpha-(BEDT-TTF)_2KHg(SCN)_4$ *Low Temp. Phys.* **37** 950–9
[18] Krstovska D, Choi E S, Steven E and Brooks J S 2012 The angular magnetothermoelectric power of a charge density wave system *J. Phys.: Condens. Matter* **24** 265502
[19] Choi E S, Brooks J S, Qualls J S and Song Y S 2001 Low-frequency method for magnetothermopower and Nernst effect measurements on single crystal samples at low temperatures and high magnetic fields *Rev. Sci. Instrum.* **72** 2392–6
[20] Qualls J S, Balicas L, Brooks J S, Harrison N, Montgomery L K and Tokumoto M 2000 Competition between Pauli and orbital effects in a charge-density-wave system *Phys. Rev.* B **62** 10008
[21] Kartsovnik M V, Zverev V N, Andres D, Biberacher W, Helm T, Grigoriev P D, Ramazashvili R, Kushch N D and Müller H 2014 Magnetic quantum oscillations in the charge-density-wave state of the organic metals $\alpha-(BEDT-TTF)_2MHg(SCN)_4$ with M = K and Tl *Low Temp. Phys.* **40** 377
[22] Krstovska D, Choi E S and Steven E 2019 Thermopower quantum oscillations in the charge density wave state of the organic conductor $\alpha-(BEDT-TTF)_2KHg(SCN)_4$ *J. Low Temp. Phys.* **195** 165

[23] Cyr-Choinière O et al 2017 Anisotropy of the Seebeck coefficient in the cuprate Superconductor $YBa_2Cu_3O_y$: Fermi-surface reconstruction by bidirectional charge order Phys. Rev. X 7 031042
[24] Qualls J S, Brooks J S, Uji S, Terashima T, Terakura C, Aoki H and Montgomery L K 2000 Temperature and angular dependence of the magnetoresistance in low dimensional organic metals arXiv:cond-mat/0005202
[25] Chaikin P M 1990 An Introduction to Thermopower for Those Who Might Want to Use It to Study Organic Conductors and Superconductors *Organic Superconductivity* ed V Z Kresin and W A Little (Boston, MA: Springer)